ELSEVIER

Journal of Organometallic Chemistry 571 (1998) 65–75

Journal of Organometallic Chemistry

Molecular and electronic structure of some silacyclopropabenzenes: the reversed Mills–Nixon effect

M. Eckert-Maksić [a,*], Z. Glasovac [a], Z.B. Maksić [b,c]

[a] *Laboratory of Physical Organic Chemistry, Ruder Bošković Institute, P.O. Box 1016, 10000 Zagreb, Croatia*
[b] *Quantum Organic Chemistry Group, Ruder Bošković Institute, P.O. Box 1016, 10000 Zagreb, Croatia*
[c] *Faculty of Science and Mathematics, Division of Physical Chemistry, The University of Zagreb, Marulićev trg 19, 10000 Zagreb, Croatia*

Received 7 May 1998; received in revised form 14 July 1998

Abstract

Molecular and electronic structure of silacyclopropabenzenes are examined by the MP3(fc)/6-31G* theoretical model. The salient feature of these compounds is alternation of bond distances of the aromatic fragment in the reversed Mills–Nixon sense i.e. the annelated CC bonds are shortened, whilst the *ortho* bonds are stretched. This is in harmony with the π-electron partial bond localization as evidenced by the π-bond order analysis, which in turn indicates that the π-effect dominates over the σ-electron rehybridization effect. Concentration of the π-density in the *ipso* bond(s) seems to be triggered by hyperconjugation with SiH_2 group(s). The latter mode of interaction is responsible for a decrease in the strain energy of silacyclopropabenzenes relative to the corresponding cyclopropabenzenes. It is shown that the total strain energy is a simple additive function of the number and types of the fused small rings involving SiH_2 group(s).

Keywords: Silacyclopraparenes; Ab initio calculations; B3LYP calculations; Bond alternations; Reversed Mills–Nixon effect

1. Introduction

Structure and properties of small ring polysilenes fused to an aromatic fragment arose continuous research interest since they exhibit unusual features as a result of a strong interplay and competition of the stabilizing aromatic and destabilizing angular strain factors [1–4]. In particular, this family of compounds shows remarkable reactivity as exemplified by unique behaviour in thermolytic and photolytic reactions [5,6]. Their importance stems from the fact that some of these compounds serve as precursors in polymer chemistry [2,3]. Recent theoretical study of disilacyclobutabenzenes revealed some interesting features of their electronic structure. For example, the average C–C distances of their aromatic perimeters are larger than the C–C bond length in a free benzene [7]. This interesting blow-up phenomenon has been rationalized by the π-electron charge transfer interaction between the highest occupied MOs of the benzene ring and the $\varphi^*(SiH_2)$ antibonding fragment orbitals of the SiH_2 groups. Hence, it seems that the σ-inductive effect of the silicon atoms, which donates electron density to the ring, is partly compensated by the π-back bonding of the aromatic moiety. Furthermore, the strain energies determined by the homodesmic reactions [8] were additive to a good approximation depending only on the number of fused four-membered rings. This is useful information regarding stability of these compounds being indicative at the same time of the relative independence of small rings, since each of them behaves practically as if others were nonexistent. In the present paper we report on the molecular and electronic structure of silacyclopropabenzenes as obtained by the high level ab initio models and by the B3LYP density func-

* Corresponding author. Fax: +385 1 425 647; e-mail: mmaksic@emma.irb.hr

0022-328X/98/$ - see front matter
PII S0022-328X(98)00858-4

tional method, which is in its nature a scaled ab initio approach (see later). The aim of this work is 2-fold: to extend the previous knowledge on arenes annelated to strained silacycloalkenes and to test the performance of the approximate but modern B3LYP scheme. In addition to silacyclopropabenzenes some of their hydrocarbon counterparts are examined too for the sake of comparison. The studied systems are depicted in Scheme 1.

2. Methodology

The density functional theory (DFT) considerably gained in its popularity recently [9]. The reason behind its success is that the corresponding methods are rather efficient being concurrently reasonably accurate. Among them the hybrid B3LYP approach deserves a particular attention in view of its simplicity and good performance. It represents a happy combination of the Hartree–Fock model and the DFT correlation correction approach. The corresponding exchange (X) and correlation functional (C) enter the E^{XC}_{hybrid} expression in the following form:

$$E^{XC}_{\text{hybrid}} = c_{\text{HF}}E^{X}_{\text{HF}} + c_{\text{DFT}}E^{XC}_{\text{DFT}} \quad (1)$$

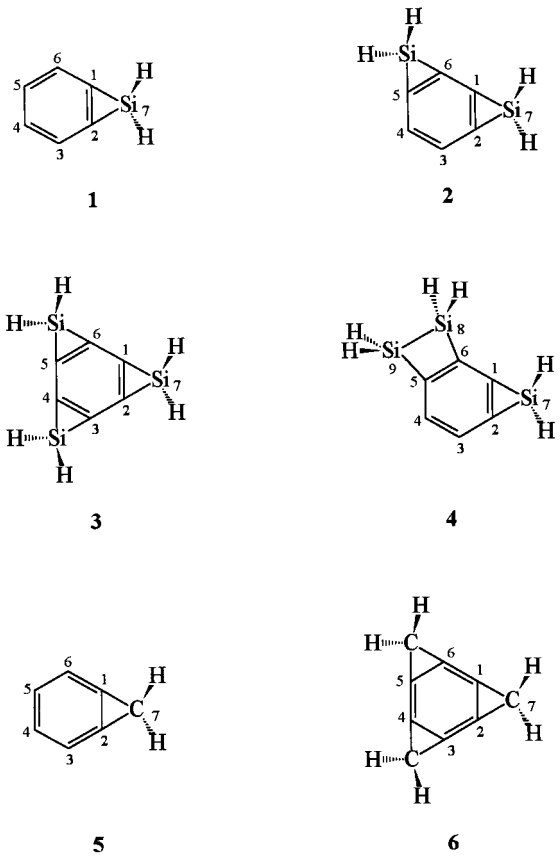

Scheme 1.

where c_{HF} and c_{DFT} are adjustable weighting factors. More specifically, the DFT-B3LYP scheme involves in fact three adjustable parameters [10]. Hence, the DFT approach is sometimes classified by some researchers as a semiempirical theory. This is not quite justified because a term semiempirical is reserved for highly approximate schemes like AM1 or PM3, where many molecular integrals are neglected, whereas others are fitted to experimental data by employing very large number of empirical weighting parameters. Since the total exchange–correlation functional (Eq. (1)) utilizes only three scaling parameters, we would like to propose a better characterization of DFT methods like the B3LYP scheme. They should be more appropriately termed as 'scaled ab initio' models.

We have previously shown that the B3LYP/6-31G* model correctly reproduces energetic properties of polyannelated silacyclobutabenzenes involving their relative stabilities and strain energies [7]. However, subtle geometric changes of the benzene fragment, induced by annelation, were better described by the MP2(fc)/6-31G* model, where the effect of electron correlation is taken into account explicitly by the Møller–Plesset perturbation theory of the second order [11]. In the present work we give results of the geometry optimizations obtained by even higher level of the theory, namely, by utilizing the MP3(fc)/6-31G* model, which employs perturbation corrections to the third order in the Møller–Plesset series. This is interesting per se since the molecular geometries of large systems at the MP3 level are sparse in the literature. More importantly, it appears that the MP3 procedure reproduces bond lengths in delocalized π-electron model systems better than the MP2 one, whereas the MP4 results offer no additional advantage for the specific 6-31G* basis set employed here. Therefore, it follows that the MP3 model is a well suited tool for studying our target molecules.

All calculations were performed by using Gaussian 94/DFT [12] and GAMESS-US [13] program packages.

3. Results and discussion

3.1. Performance of the selected model

Theoretical model of choice should be feasible, economical and reliable. Concomitantly, it should offer results which could be interpreted in terms of simple and qualitative, but general concepts widely applicable in rationalizing the basic facets of the chemical bonding. It is not easy to reconcile all these requirements. Earlier work has shown that the MP2(fc)/6-31G* model describes fairly well structural distortions of the aro-

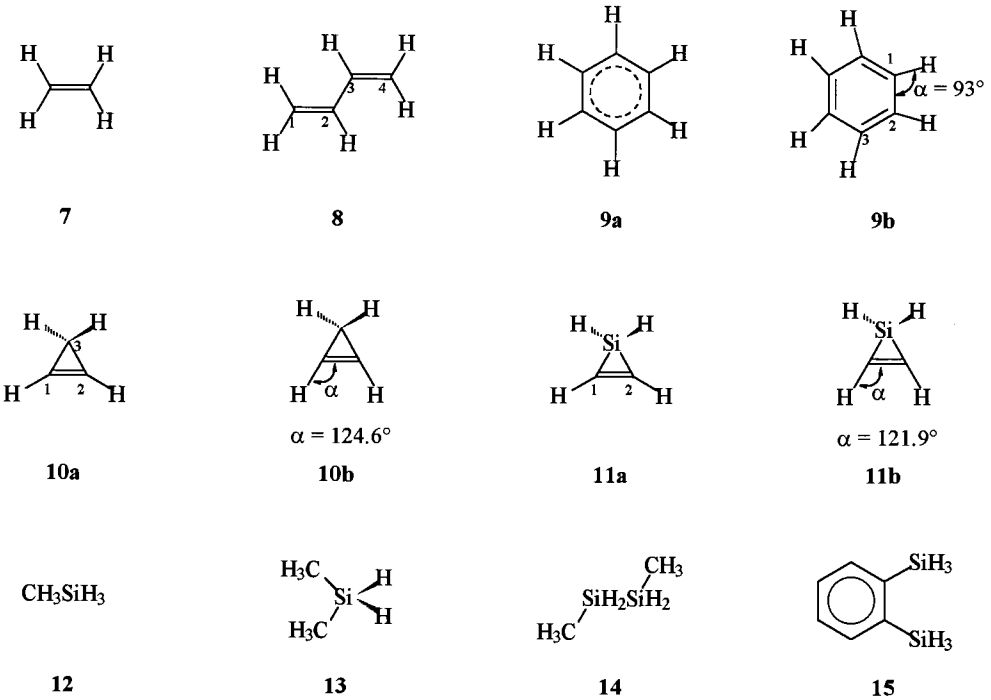

Scheme 2.

matic moiety induced by fusion of small hydrocarbon rings as well as their electron density distributions [14–16]. The same holds for fused silacyclobutabenzenes [7]. However, geometries, electronic structure and energetics of planar systems involving CC double or triple bonds require use of highly intricate ab initio methods [17,18]. Consequently, we shall examine performance of the MPn(fc)/6-31G* models ($n = 2$, 3 and 4) in reproducing structural features of a set of the carefully selected small model compounds encompassing ethylene, *trans*-butadiene, benzene, cyclopropene, silacyclopropene and some of their deliberately deformed structures (Scheme 2). They represent delocalized π-systems and/or important fragments of the target fused compounds. Perusal of the presented data in Table 1 shows that MPn and B3LYP models yield bond distances in a good agreement with observed data. However, MP3 results are definitely better than the MP2 and B3LYP calculated CC distances in 1,3-butadiene, which represents a prototype of a weakly π-electron delocalized system. The same holds for cyclopropene **10a**. It is also important to notice that MP4 approach does not offer any significant advantage over the MP3 level for the examined small compounds and the given 6-31G* basis set. This is encouraging since the latter model is feasible in molecular systems under scrutiny. Hence, one can safely conclude that the MP3(fc)/6-31G* model provides a suitable vehicle in exploring structural features of silacyclopropabenzenes.

3.2. The spatial and electronic structure of silacyclopropabenzenes

Selected geometrical parameters of silacyclopropabenzenes **1**–**4** are presented in Table 2, where they are compared with the structures of the corresponding hydrocarbons **5** and **6**. In what follows we shall discuss MP3 results first. Survey of the given data reveals that fusion of small silacyclopropenes induces bond lengths alternation within the benzene moiety. It appears that C(1)=C(2), C(3)=C(4) and C(5)=C(6) bond distances are shorter than the benzene CC bond length (1.395 Å), whereas the remaining bonds are elongated sometimes quite appreciably as in **3** (1.420 Å). This feature is characteristic for the anti-Mills–Nixon bond fixation (vide infra). The opposite takes place in cyclopropabenzene **5** and tris-cyclopropabenzene **6**, which is compatible with the original Mills–Nixon assumption [24]. Bond fixation within the benzene moiety is reflected in the bond localization index defined as:

$$L_{\mathrm{m}}(d) = \sum_{n} |d_{\mathrm{CC}}^{(n)} - \bar{d}_{\mathrm{CC}}| / \text{Å} \qquad (2)$$

where $\bar{d}_{\mathrm{CC}}$ denotes the average CC bond distance of the six membered ring and summation is extended over the aromatic perimeter. Further, m stands for the molecule in question, whilst n signifies a particular CC bond within a ring [25]. The increase in $L_{\mathrm{m}}(d)$ describes the bond localization effect, which is exactly zero for the perfectly aromatic benzene. An analogous expression holds for the π-bond orders:

Table 1
Comparison of selected geometrical parameters in model molecules **7**–**11** as predicted by several theoretical methods with the available experimental data (Å)

Molecule	Bond r (Å)	B3LYP/6-31G*	MP2(fc)/6-31G*	MP3(fc)/6-31G*	MP4(sdq)/6-31G*	Exptl.
7	C–C	1.331	1.336	1.334	1.337	1.337[a]
8	C(1)–C(2)	1.341	1.344	1.340	1.343	1.343[b]; 1.342[c]
	C(2)–C(3)	1.457	1.458	1.465	1.465	1.467; 1.463
9a	C–C	1.397	1.397	1.395	1.397	1.396[d]
9b	C(1)–C(2)	1.498	1.488	1.502	1.505	
	C(2)–C(3)	1.355	1.363	1.352	1.352	
10a	C(1)–C(2)	1.295	1.303	1.297	1.300	1.296[e]
	C(2)–C(3)	1.509	1.507	1.508	1.509	1.509
10b	C(1)–C(2)	1.307	1.316	1.309	1.313	
	C(2)–C(3)	1.508	1.506	1.508	1.510	
11a	C(1)–C(2)	1.336	1.344	1.338	1.342	
	C(2)–Si	1.822	1.820	1.820	1.822	
11b	C(1)–C(2)	1.349	1.360	1.352	1.356	
	C(2)–Si	1.811	1.807	1.807	1.810	

References: [a] [19]; [b] [20]; [c] [21]; [d] [22]; [e] [23].

$$L_m(\pi) = \sum_n |\pi_{CC}^{(n)} - \bar{\pi}_{CC}^{(n)}| \quad (3)$$

where the notation has its obvious meaning. Employing results summarized in Table 2 one obtains $L_m(d)$ values 0.04, 0.08 and 0.10 for molecules **1**, **2** and **3**, respectively. The corresponding $L_m(\pi)$ values are 0.31, 0.57 and 0.78. It follows that the bond fixation and the accompanying aromaticity defect increase almost linearly along the series. It is interesting to notice a small but steady increase of the average CC bond distance in the same direction. They assume values 1.398, 1.400 and 1.403 Å, respectively, thus exhibiting considerably smaller blow up effect relative to silacyclobutabenzenes [7]. Obviously, this is a consequence of a smaller number of Si atoms. This conclusion is supported by the average d(CC) bond distances of 1.404 Å in **4**, which is larger than that in **2**. Interestingly enough, hydrocarbon counterparts **5** and **6** behave differently. Fusion of cyclopropyl ring(s) leads to the benzene fragment contraction as evidenced by the average d(CC) bond distances in **5** and **6** of 1.389 and 1.370 Å, respectively. There are some other notable differences. In silacyclopropabenzenes the annelated bonds are shorter than in the free benzene, whereas the opposite is the case with *ortho*- (and *para*-) bonds. Concomitantly, *meta*- bonds are shrunk too in addition to the *ipso* ones. This effect obviously increases along the series **1**–**3** and it is nicely reproduced by the π-bond orders (Table 3). As an illustrative example we mention that the π-b.o. value in the fused bond in **3** is 0.73 thus being higher by 0.26 than the *ortho* bond. Hence, there is an apparent similarity between the CF_2 groups in polyfluorocyclopropa(cyclobuta)benzenes [7,14,26] and SiH_2 groups in the corresponding sila-derivatives since they both concentrate π-density in the annelated bonds. This seemingly counterintuitive charge drift deserves a closer scrutiny. It is well known by now that fusion of small rings to the aromatic moiety causes rehybridization at the carbon junction atoms [7,14,15,26,27], leading to a shift of the s-character from the annelated to the adjacent *ortho* bonds. As a typical example we consider a deformed benzene **9b**, where a tormented aromatic nucleus exhibits pronounced bond alternation (Table 2). This is a clear cut case, where changes in the σ-plane trigger a redistribution of the π-density in a plane perpendicular to the aromatic moiety passing through a pair of bonded C atoms. More specifically, redistribution of the σ-density upon fusion (the angular strain effect) induces migration of the π-electron density in the same direction-from the *ipso* (annelated) to the *ortho* bonds. Concomitantly, the *ipso* and the *ortho* bonds are described by the average s-characters of 27.9 and 41.0%, respectively, whereas the corresponding π-bond orders are 0.50 and 0.79, thus being in harmony with the Mills–Nixon (MN) hypothesis. It is also important to stress that σ- and π-densities are distributed in concerted and synergistic manner leading to a pronounced difference between $d(CC)_i$ and $d(CC)_o$ being as high as 0.15 Å, where subscripts i and o stand for *ipso* and *ortho* bonds, respectively. An opposite π-electron localization pattern occurs in the so called reversed MN case as exemplified by the edge protonated o-benzyne [29]. In anti-MN systems the π-density of the *ipso* bond is increased in an apparent tendency to shield the positive charge in the edge protonated o-benzyne and/or to enhance the aromatic character of the three-membered ring in benzocyclopropenyl cation. A similar situation takes place in fluorocyclopropabenzenes and silacyclopropabenzenes, where CH_2 fragments are replaced by CF_2 or SiH_2 groups. The p-atomic orbital of carbon/silicon atom in these groups, which is perpendicular to the molecular plane, has a low electron

Table 2
Selected structural parameters of compounds **1**–**6**

Parameters	**1**	**2**	**3**	**4**	**5**	**6**
Bond r(Å)						
C(1)–C(2)	1.398	1.397	1.398	1.395	1.352	1.384
	1.401	1.402	1.406	1.402	1.352	1.379
	[1.392]	[1.387]	[1.385]	[1.389]	[1.348]	[1.377]
C(2)–C(3)	1.397	1.408	1.408	1.402	1.380	1.361
	1.397	1.408	1.405	1.401	1.382	1.369
	[1.401]	[1.416]	[1.420]	[1.406]	[1.380]	[1.363]
C(1)–C(6)	1.397	1.399	1.408	1.402	1.380	1.361
	1.397	1.399	1.405	1.401	1.382	1.369
	[1.401]	[1.408]	[1.420]	[1.407]	[1.380]	[1.363]
C(3)–C(4)	1.395	1.395	1.398	1.395	1.412	1.384
	1.396	1.397	1.406	1.397	1.409	1.379
	[1.390]	[1.386]	[1.385]	[1.388]	[1.410]	[1.377]
C(6)–C(5)	1.395	1.397	1.398	1.423	1.412	1.384
	1.396	1.402	1.406	1.426	1.409	1.379
	[1.390]	[1.387]	[1.385]	[1.413]	[1.410]	[1.377]
C(4)–C(5)	1.410	1.408	1.408	1.414	1.404	1.361
	1.411	1.408	1.405	1.414	1.408	1.369
	[1.414]	[1.416]	[1.420]	[1.419]	[1.404]	[1.363]
C(1)–Si(C)	1.821	1.821	1.825	1.825	1.503	1.505
	1.821	1.823	1.829	1.824	1.503	1.507
	[1.817]	[1.816]	[1.820]	[1.818]	[1.506]	[1.509]
C(2)–Si(C)	1.821	1.827	1.825	1.825	1.503	1.505
	1.821	1.828	1.829	1.826	1.503	1.507
	[1.817]	[1.821]	[1.820]	[1.821]	[1.506]	[1.509]
Angle (°)						
C(2)–C(1)–C(6)	121.9	118.4	120.0	121.7	124.4	120.0
	122.0	118.3	120.0	121.5	124.6	120.0
	[121.9]	[118.3]	[120.0]	[121.5]	[124.6]	[120.0]
C(1)–C(6)–C(5)	116.4	118.4	120.0	116.2	113.3	120.0
	116.3	118.3	120.0	116.2	113.0	120.0
	[116.4]	[118.3]	[120.0]	[116.4]	[113.0]	[120.0]
C(1)–C(2)–C(3)	121.9	123.4	120.0	122.3	124.4	120.0
	122.0	123.5	120.0	122.4	124.6	120.0
	[121.9]	[123.5]	[120.0]	[122.4]	[124.6]	[120.0]
C(2)–C(3)–C(4)	116.4	118.2	120.0	117.0	113.3	120.0
	116.3	118.2	120.0	117.0	113.0	120.0
	[116.4]	[118.2]	[120.0]	[117.0]	[113.0]	[120.0]
C(4)–C(5)–C(6)	121.7	123.4	120.0	121.7	122.3	120.0
	121.8	123.5	120.0	121.5	122.5	120.0
	[121.7]	[123.5]	[120.0]	[121.6]	[122.4]	[120.0]
C(3)–C(4)–C(5)	121.7	118.2	120.0	121.3	122.3	120.0
	121.8	118.2	120.0	120.0	122.5	120.0
	[121.7]	[118.2]	[120.0]	[121.1]	[122.4]	[120.0]
C(1)–Si(C)–C(2)	45.2	45.4	45.0	45.0	53.4	54.8
	45.2	45.6	45.2	45.2	53.4	54.5
	[45.0]	[45.2]	[45.0]	[44.8]	[53.2]	[54.2]

Triplets of numbers in each column refer to results of the B3LYP, MP2(fc)/6-31G* and MP3(fc)/6-31G* methods, respectively. Results of the adopted MP3 model are given within the square parentheses.

population in view of the higher electron withdrawing power of the more electronegative fluorine/hydrogen atoms. Consequently, the hyperconjugative interaction within the three-membered ring(s) is favorable leading to reinforcement of π-density in the *ipso* (fused) CC bond(s). This is reflected also in the C–Si π-bond orders which assume values in the range 0.23–0.26. The upper limit is reserved for silacyclopropene **11a** which should be compared to the C–C π-b.o. in cyclopropene **10a** of 0.16. It follows as a corollary that σ- and π-densities in silacyclopropabenzene are distributed in disconcerted and antagonistic way. Apparently, the influence of the π-density prevails yielding a shortening of the *ipso* bonds in spite of their low s-character.

An additional insight into the charge distribution in molecules is offered by the Bader's topological analysis based on the theory of atoms in molecules [30]. Useful bonding information are stored in the bond critical

Table 3
Bonding parameters and AIM electron distribution indices as extracted from MP3(fc)/6-31G* wavefunctions[a]

Bond	s (%)	Löwdin	Bader	AIM indices		
		π-b.o.	Total b.o.	ε	ρ_c	$\nabla^2\rho_c$
1						
C(1)–C(2)	29.3–29.3	0.65	1.740	0.073	0.317	−0.818
C(2)–C(3)	41.5–34.1	0.58	1.143	0.140	0.302	−0.818
C(3)–C(4)	35.4–35.8	0.71	1.600	0.247	0.316	−0.880
C(4)–C(5)	34.8–34.8	0.60	1.143	0.189	0.302	−0.822
C(1)–Si(7)	28.9–21.4	0.23	0.470	0.508	0.109	0.386
C(3)–H	30.5	—	0.955	0.016	0.277	−0.978
C(4)–H	29.3	—	0.952	0.014	0.276	−0.968
Si(7)–H	28.5	—	0.545	0.036	0.117	0.154
2						
C(1)–C(2)	29.3–30.1	0.69	1.754	0.096	0.320	−0.831
C(1)–C(6)	40.5–40.5	0.51	1.126	0.067	0.292	−0.761
C(2)–C(3)	41.1–33.9	0.53	1.124	0.114	0.294	−0.781
C(3)–C(4)	36.0–36.0	0.76	1.619	0.269	0.317	−0.882
C(1)–Si(7)	29.8–21.4	0.23	0.469	0.481	0.109	0.385
C(2)–Si(7)	28.6–21.3	0.24	0.466	0.515	0.108	0.380
C(3)–H	30.1	—	0.953	0.015	0.276	−0.981
Si(7)–H	28.6	—	0.545	0.035	0.117	0.152
3						
C(1)–C(2)	30.0–30.0	0.73	1.763	0.112	0.321	−0.831
C(1)–C(6)	40.3–40.3	0.47	1.114	0.045	0.286	−0.735
C(1)–Si(7)	29.4–21.3	0.24	0.466	0.485	0.108	0.380
Si(7)–H	28.7	—	0.564	0.036	0.118	0.152
4						
C(1)–C(2)	29.3–29.6	0.67	1.742	0.079	0.319	−0.827
C(1)–C(6)	41.7–35.4	0.55	1.142	0.098	0.298	−0.795
C(2)–C(3)	41.3–33.9	0.56	1.134	0.126	0.300	−0.808
C(3)–C(4)	35.7–35.6	0.73	1.603	0.250	0.317	−0.883
C(4)–C(5)	35.0–36.2	0.56	1.141	0.144	0.298	−0.800
C(5)–C(6)	34.0–33.4	0.68	1.617	0.183	0.304	−0.797
C(1)–Si(7)	28.7–21.5	0.23	0.472	0.494	0.109	0.381
C(2)–Si(7)	28.8–21.2	0.23	0.467	0.524	0.108	0.383
C(5)–Si(9)	29.7–23.6	0.19	0.525	0.053	0.111	0.272
C(6)–Si(8)	31.2–23.6	0.19	0.527	0.053	0.112	0.279
Si(8)–Si(9)	23.5–23.8	0.09	0.741	0.010	0.091	−0.153
C(3)–H	30.3	—	0.954	0.015	0.277	−0.981
C(4)–H	29.3	—	0.951	0.014	0.276	−0.968
Si(7)–H	28.7	—	0.546	0.037	0.117	0.153
Si(8)–H	26.4	—	0.580	0.034	0.114	0.156
Si(9)–H	26.3	—	0.580	0.035	0.114	0.157
5						
C(1)–C(2)	25.7–25.7	0.62	1.149	0.056	0.342	−0.957
C(2)–C(3)	43.7–33.6	0.66	1.585	0.204	0.308	−0.829
C(3)–C(4)	35.2–35.1	0.64	1.151	0.228	0.304	−0.822
C(4)–C(5)	35.6–35.6	0.67	1.583	0.232	0.306	−0.830
C(1)–C(7)	30.4–21.0	0.17	0.977	0.557	0.230	−0.349
C(3)–H	31.2	—	0.957	0.019	0.276	−0.978
C(4)–H	29.2	—	0.952	0.018	0.276	−0.964
C(7)–H	28.9	—	0.952	0.015	0.274	−0.946
6						
C(1)–C(2)	24.6–24.6	0.57	1.107	0.052	0.323	−0.839
C(1)–C(6)	43.2–43.2	0.69	1.624	0.174	0.302	−0.749
C(1)–C(7)	32.0–21.0	0.16	0.980	0.468	0.228	−0.360
C(7)–H	29.0	—	0.949	0.012	0.274	−0.953
7						
C–C	39.4–39.4	0.99	1.874	0.400	0.343	−1.000
C–H	30.3	—	0.969	0.014	0.275	−0.962

Table 3 (Continued)

Bond	s (%)	Löwdin	Bader	AIM indices		
		π-b.o.	Total b.o.	ε	ρ_c	$\nabla^2\rho_c$
9a						
C(1)–C(2)	35.1–35.1	0.66	1.371	0.220	0.312	−0.869
C(1)–H	29.7	—	0.947	0.016	0.276	−0.965
9b						
C(1)–C(2)	27.9–27.9	0.50	1.060	0.140	0.259	−0.583
C(2)–C(3)	41.0–41.0	0.79	1.704	0.276	0.327	−0.931
C(1)–H	31.1	—	0.940	0.007	0.277	−0.972
10a						
C(1)–C(2)	35.8–35.8	0.95	1.862	0.247	0.349	−0.923
C(1)–C(3)	24.6–20.3	0.16	1.010	0.613	0.233	−0.338
C(1)–H	39.4	—	0.973	0.003	0.275	−1.007
C(3)–H	29.7	—	0.969	0.035	0.273	−0.926
10b						
C(1)–C(2)	28.2–28.2	0.94	1.864	0.222	0.360	−1.016
C(1)–C(3)	31.6–20.3	0.16	1.008	0.663	0.225	−0.299
C(1)–H	40.0	—	0.965	0.004	0.267	−0.933
C(3)–H	29.6	—	0.964	0.021	0.276	−0.955
11a						
C(1)–C(2)	35.0–35.0	0.90	2.016	0.187	0.337	−0.894
C(1)–Si(3)	26.5–20.4	0.26	0.502	0.558	0.109	0.399
C(1)–H	38.2	—	0.952	0.017	0.271	−0.959
Si(3)–H	29.5	—	0.550	0.062	0.116	0.158
11b						
C(1)–C(2)	30.9–30.9	0.89	1.980	0.172	0.336	−0.896
C(1)–Si(3)	30.9–21.0	0.27	0.477	0.538	0.108	0.415
C(1)–H	37.9	—	0.943	0.019	0.270	−0.940
Si(3)–H	29.0	—	0.541	0.043	0.117	0.155

[a] The atom in molecules indices are abbreviated as AIM.

points (bcp) which correspond to a minimum of the electron density on its ridge connecting two bonded atoms. Density ρ_c at the bcp has a property that $\nabla\rho_c = 0$ and that it is a saddle point. The latter implies that it has two negative curvatures λ_1 and λ_2, whilst the third (λ_3) related to the pathway along the ridge, is positive. The potential π-character of the bond is defined by its elipticity $\varepsilon = (\lambda_1/\lambda_2 - 1)$. The bond order in Bader's zero density flux theory of atoms in molecules is given by n:

$$n_c = \exp[A(\rho_c - B)] \quad (4)$$

where A and B are deliberately selected constants, which ascribe bond order 2 and 3 to the CC bonds in ethylene and acetylene, respectively. It is noteworthy that n_c of benzene is 1.6. Elipticity of CC bonds in benzene and ethylene are 0.22 and 0.40, respectively, implying that the former molecule is fairly well described by two valence bond Kekulé structures. It is important to point out that elipticity of the angularly strained double bond is low [15], because bent chemical bonds have some π-character too. However, the π-ellipticity of the double bond is somewhat higher ($\lambda_1 > \lambda_2$) leading to small positive values of ε.

Finally, Laplacian of the electron density $\nabla^2\rho_c$ gives some indication about the strength of the covalent bond. The more negative $\nabla^2\rho_c$, the larger is a lump of the electron density between the bonded atoms and, consequently, the more tight chemical bonding occurs as a rule. We shall compare these qualitative indices with the total Bader bond order $B(bo)_t$, Table 3. Perusal of the MP3 results shows that the annelated bonds exhibit a steady increase in ε along the series **1–3** in accordance with increase in their π(bo) as expected. Conversely, ε and π(bo) decrease in adjacent C(2)–C(3) bonds. It is noteworthy that *meta* C(3)–C(4) bonds in **1** and **2** have ε values 0.247 and 0.269, respectively, thus possessing more localized π-bonds than benzene (ε = 0.22). Laplacian $-\nabla^2\rho_c$ is the lowest for C(3)–C(4) bonds **1** and **2** indicating that they are the strongest bonds in these compounds. This conjecture is supported by the relatively high s-character and a pronounced π-bond order. Somewhat unexpectedly, $B(bo)_t$ value is the highest for annelated bonds, which is difficult to

Table 4
Atomic charges extracted from MP3(fc)/6-31G* wavefunctions by using various density partitioning recipes

Atoms	Löwdin	Mull.	NBO	Bader	Löwdin	Mull.	NBO	Bader
	1[a]				**5**[b]			
C(1)	−0.17	−0.13	−0.43	−0.74	−0.06	0.03	−0.04	−0.16
C(3)	−0.14	−0.17	−0.21	−0.01	−0.15	−0.20	−0.23	0.01
C(4)	−0.15	−0.17	−0.22	−0.04	−0.16	−0.18	−0.23	−0.04
X(7)	0.31	0.42	1.16	2.75	−0.25	−0.39	−0.42	0.05
H(C3)	0.17	0.18	0.23	0.06	0.17	0.18	0.23	0.04
H(C4)	0.17	0.18	0.24	0.05	0.16	0.17	0.24	0.05
H(Si7)	−0.02	−0.10	−0.19	−0.69	0.16	0.18	0.23	0.06
	3[a]				**6**[b]			
C(1)	−0.14	−0.12	−0.40	−0.69	−0.05	0.01	−0.03	−0.10
X(7)	0.32	0.43	1.18	2.75	−0.23	−0.39	−0.42	0.07
H(Si)	−0.02	−0.09	−0.19	−0.69	0.17	0.19	0.24	0.06

[a] X = Si; [b] X = C.

reconcile with their significant bent bonding and rather low average s-character. We conclude that Bader's total bond order is not a good criterion of the bonding strength if the compared bonds greatly differ in their bent bond character. Concomitantly, $B(bo)_t$ should be used as a bonding index with a due caution. Since all bonding indices except the s-character are strongly in favour of the annelated bond in **3**, we are tempted to say that fused bonds are more tightly bound than *ortho* CC bonds. The opposite seems to be the case in **6**. It is also safe to assert that *ortho* bonds are substantially stronger than 'fused' CC bonds in **9b**.

Interpretation of the bond distances in cyclopropabenzene and their silacyclopropabenzene counterparts is not an easy task. Strictly speaking one should distinguish between the interatomic bond distance (IBD) corresponding to the length associated with the straight line passing through the directly linked nuclei and the bond path length (BPL) defined on the (curved) ridge of the maximum electron density. These two types of bond distances generally do not differ dramatically, but they are significantly diverse in the highly strained three-membered rings [15]. It is well known that the annelated CC bond in cyclopropabenzenes is strongly bent inside the aromatic ring. Therefore, this particular bond should not be compared with the CC bond in free benzene. Instead, it should be gauged e.g. by the C=C bond distance in cyclopropene, because the latter has similar bent bond character.

In what follows we shall discuss IBDs. The CC double bond distance in **11a** is 1.338 Å implying that the annelated bond in **1** is enlarged by fusion roughly by 0.05 Å. In order to delineate rehybridization and π-electron effects we consider synchronous deformation of CH bonds in **11b**, which mimics annelation to the benzene ring. It leads to an increase in CC distance by 0.014 Å. It follows that additional lengthening of 0.011 Å is caused by a decrease in π(bo) from 0.89 to 0.65 found in **11a** and the parent molecule **1**, respectively. Hence, the annelated bond distance is increased according to the adopted criterion in spite of the shift of the π-density toward this bond as a consequence of the reversed MN effect. This increase would be even higher if the anti-MN effect was not present. For that reason it was pointed out that the *ortho* bond is usually better indicator of the underlying mechanism operating in fused systems [15]. Their shrinkage or stretching is an obvious mark of the MN or anti MN effect of the fused small ring(s) on the aromatic nucleus. It follows that compounds **1**–**4** are anti-MN systems, whereas **5** and **6** exhibit MN type of the π-electron bond fixation and a concomitant geometric distortion. It should be pointed out that fusion of small ring introduces some angular deformation of the benzene fragment too. For instance, C(1)–C(6)–C(5) and C(6)–C(5)–C(4) in **1** are 116.4° and 121.7°, respectively. It is noteworthy that their deviations from the ideal 120° are significantly lower than in **5** (Table 3).

Finally, a word on the atomic charges is in place here. For this purpose we list in Table 4. formal charges of some selected systems **1**, **3**, **5** and **6** as obtained by four recipes: Löwdin symmetric orthogonalization, classical Mulliken population analysis, natural bond orbital analysis and Bader's atomic domains densities [31]. It appears that Löwdin's populations correspond to very moderate interatomic charge transfer thus being closest to intuition. On the other hand, Bader's charges grossly overestimate electron density drift even in the starting promolecule, where noninteractive atoms are placed at the equilibrium positions [31]. Consequently, they are less realistic. Comparing atomic charges in silacyclopropabenzenes with their hydrocarbon counterparts one observes a notable difference at the carbon junction atoms in the former compounds since they become more negative. This is a consequence of the Si σ-electron donation. Negative charges of the remaining C

atoms originate from the electron densities transferred from hydrogens. A point of considerable interest is a comparison of the π-density of the carbon junction atoms in **3** and **6**. It is 0.90 |e| in the former molecule despite the fact that the total atomic charge is negative (-0.14 |e|). The π-electron population in **6** is higher being 0.96 |e|. This finding is in harmony with the π-back bonding via the hyperconjugative mechanism in molecules **1**–**3** as discussed earlier.

3.3. Molecular strain energies

Strain energies are most conveniently estimated by the hypothetical homodesmic reactions. These reactions are designed to match number and types of chemical bonds in reactants and products preserving at the same time at least approximately the hybridization states of the interacting atoms [8]. Typical homodesmic reaction(s) related to the destabilization energy of silacyclopropabenzenes is given by:

$$\boldsymbol{n} + 2N * (CH_3SiH_3) + (N-1)\ \text{benzene} = N * 15 + N(CH_3SiH_2CH_3) \quad (5)$$

where ***n*** stands for compounds **1**, **2** and **3**, whereas N denotes number of three-membered rings. Analogously, the angular strain of silacyclopropene is defined by:

$$11\mathbf{a} + 2N * (CH_3SiH_3) = CH_3SiH_2CH_3 + SiH_3CH{=}CHSiH_3 \quad (6)$$

where $SiH_3CH{=}CHSiH_3$ is taken in its most stable E conformation. The corresponding energies are $-$659.98065 and $-$658.60061 a.u. for B3LYP and MP2(fc)/6-31G* methods, respectively. Molecular energies necessary for calculation of the strain energy are given in Table 5. It is instructive to compare silacyclopropabenzenes **1** and **3** with their counterparts **5** and **6**. The MP2 model (Table 6) unequivocally shows that cyclopropabenzenes are considerably more strained systems. The same holds for **10a** as compared to **11a** the difference being 13.6 kcal mol^{-1}. A plausible explanation is given by the pronounced hyperconjugative interaction in silacyclopropene and related compounds. Another point of interest is that silacyclopropabenzene **1** is somewhat more strained than **11a** by 6 kcal mol^{-1}, which can be rationalized by deformation of the silacyclopropene ring upon fusion. This effect can be estimated by bending C–H bonds in **11a** in a way leading to **11b**, where $\alpha = 121.9°$ is the angle found in the prototypical compound **1**. It implies a decrease in the H–C(1)–C(2) angle by 14°. Clearly, the bending deformation increases H···H repulsion which does not occur in **1**. Hence, we shall subtract H(C1)···H(C2) repulsion in **11a** and **11b** in a simple point charge approximation in order to extract pure electronic effect. Employing Löwdin charges one obtains an increase in Coulomb repulsion of 3.5 kcal mol^{-1}. A difference in E_{tot} between **11b** and **11a** is 5.3 kcal mol^{-1} implying that about 2 kcal mol^{-1} is due to an increase in the electronic energy. Taking into account that **1** is more strained than a free silacyclopropene **11a** by 6 kcal mol^{-1}, it follows that about 4 kcal mol^{-1} is due to a decrease in the hyperconjugative interaction in the former molecule. This is clearly reflected in the corresponding C(1)–Si π-bond orders, which in **1** and **11a** assume values 0.23 and 0.26, respectively (Table 3). It should be kept in mind that the foregoing analysis is only qualitatively valid, since there is a small spill-over of the angular strain from the three-membered ring to the aromatic fragment too as exemplified e.g. in the C(1)–C(6)–C(5) angle of 116.4° in **1** (Table 3). This is much more pronounced in **5**, where the corresponding

Table 5
Total energies (E_{tot}) in a.u. of the investigated silacyclopropabenzenes and model compounds necessary for homodesmic reactions (**5**) and (**6**)

Molecule	B3LYP/6-31G*	MP2(fc)/6-31G*	MP3(fc)/6-31G*
1	−521.67558	−520.38610	−520.41339
2	−811.10132	−809.31326	−809.33899
3	−1100.52722	−1098.24072	−1098.26408
4	−1101.84707	−1099.52219	−1099.56139
5	−270.25694	−269.35357	−269.37859
6	−346.26275	−345.13255	−345.14788
7	−78.58746	−78.28503	−78.30598
8	−155.99214	−155.42265	−155.45571
9a	−232.24866	−231.45773	−231.48624
9b	−232.08679	−231.29018	−231.31774
10a	−116.61904	−116.20525	−116.22611
10b	−116.59280	−116.17736	−116.19783
11a	−368.02824	−367.22427	−367.24768
11b	−368.02007	−367.21583	−367.23918
12	−331.21088	−330.48523	−330.51370
13	−370.53795	−369.66395	−369.70235
14	−661.23464	−659.81997	−659.87219
15	−813.63361	−811.77159	−811.81817

Table 6
Strain energies estimated by the homodesmic reactions (**5**) and (**6**) employing B3LYP/6-31G* and MP2(fc)/6-31G* results (in kcal mol^{-1})

Molecule	B3LYP/6-31G*	Add.	MP2(fc)/6-31G*	Add.
1	46.6	—	49.6	—
2	93.9	93.9	99.9	99.2
3	141.1	139.8	150.0	148.8
4	63.1	63.3	66.7	65.9
5	69.4	—	71.3	—
6	214.9	—	217.1	213.9
10a	57.3	—	57.4	—
11a	43.0	—	43.8	—

angle becomes more acute (113°). A similar analysis as outlined above shows that the increase in the electronic energy in deformed cyclopropene **10b** is 11.4 kcal mol^{-1} meaning that an amount of 4 kcal mol^{-1} is left in **5** for the angular strain spill-over effect.

Finally, a brief comment on the additivity of the strain energy is in place here. It appears that E_s in **2** and **3** is obtained simply by multiplying the strain energy of **1** ($\approx$ 50 kcal mol^{-1}) by the number of small strained rings. A similar conclusion holds for **6**, where the total strain of 217 kcal mol^{-1} is closely reproduced by the additivity rule which yields 214 kcal mol^{-1}. An intuitively appealing explanation is found in the high transferability of the bonding parameters between the corresponding fragments within the same molecule and along the family of related molecules (Table 3).

4. Conclusion

The main result of the present analysis is anisotropy and alternation of CC bond lengths in silacyclopropabenzenes as obtained by the MP3 model. Both B3LYP and MP2 calculations do not offer a consistent picture. This finding casts some doubts on earlier premature conjectures based on inadequate models that fusion of small ring(s) does not introduce any significant distortion of the benzene fragment. Deformation of the benzene ring in systems **1**–**3** is indicative of the reversed MN effect, which is confirmed by the π-electron density analysis which reveals its considerable concentration on the annelated bonds. It is also shown that the central aromatic moiety is slightly enlarged by the hyperconjugative interaction with SiH_2 group(s). The latter mechanism is responsible for a decrease in the strain energy of silacyclopropabenzenes relative to their cyclopropabenzene counterparts. On the other hand, the strain energy of silacyclopropabenzenes is larger than that of the corresponding small ring silacyclopropene. This can be rationalized by the additional distortion of the fused three-membered ring upon annelation and the induced aromaticity defect following partial π-electron localization. It is possible that antagonistic distributions of σ- and π- electrons has a contribution to the overall destabilization too. Nevertheless, it seems that silacyclopropabenzenes are prone to chemical synthesis, since their destabilization energies are moderate. It appears also that the strain energy is an additive function of the number and types of the annelated small rings.

In conclusion, we should like to stress that the Mills–Nixon effect proved useful in interpreting the experimentally established regioselectivity in the electrophilic aromatic substitution reactions of annelated systems [32,33], in rationalizing distribution of the spin density measured by the ESR technique [34,35] and, last but not least, in predicting relative stability of tautomers of annelated systems [36,37]. It is also interesting to point out that buckminsterfullerene is the Mills–Nixon system par excellence, where the bond length alternation of deformed benzene fragment is caused predominantly by the fused five-membered rings [38] as evidenced by both the X-ray [39] and ED measurements [40].

The reversed MN systems are less abundant and their properties are not well understood as yet. It is clear, however, that their electrophilic reactivity exhibits exactly the opposite pattern than MN-compounds [28]. Recently, the reversed MN distribution and alternation of CC bonds was observed in $Fe(CO)_3$ complex of benzocyclobutadiene by the X-ray measurements [41]a. We note for the record that earlier ^{13}C measurements of cyclobutabenzene chromium tricarbonyl complexes provided some evidence on the partial π-bond localization and MN deformation of the benzene ring [41]b. It is hoped that presented results on silacyclopropabenzenes will encourage additional studies of these interesting compounds and related systems.

Acknowledgements

This work was supported by the Ministry of Science and Technology of the Republic of Croatia through projects Nos. 00980801 and 00980803. Our thanks go to The Center for Advanced Computations of the University of Zagreb for donation of the computer time.

References

[1] (a) T.J. Barton, J.A. Kilgour, J. Am. Chem. Soc. 98 (1976) 7746. (b) D. Seyferth, S.C. Vick, J. Organomet. Chem. 125 (1977) C11. (c) H. Sakurai, T. Kobayashi, Y. Nakadaira, J. Organomet. Chem. 162 (1978) C43. (d) M. Ishikawa, H. Sugishawa, M. Kumada, H. Kawakami, T. Yamabe, Organometallics 2 (1983) 974. (d) M.J. Fink, J. Deyoung, R. West, J. Michl, J. Am. Chem. Soc. 105 (1983) 1070. (e) C.H. Lin, C.Y. Lee, C.S. Liu, J. Am. Chem. Soc. 108 (1986) 1323. (f) C.Y. Lee, C.S. Liu, J. Organomet. Chem. 469 (1994) 151.

[2] M. Ishikawa, A. Naka, Synlett, (1995) 794 and the references cited therein.

[3] K. Shiina, J. Organomet. Chem. 310 (1986) C57.

[4] M. Ishikawa, H. Sakamoto, T. Tabuchi, Organometallics 10 (1991) 3173.

[5] A. Naka, M. Hayashi, S. Okazaki, M. Ishikawa, Organometallics 13 (1994) 4994.

[6] H. Sakamoto, M. Ishikawa, Organometallics 11 (1992) 2580.

[7] M. Eckert-Maksić, Z. Glasovac, M. Hodošček, A. Lesar, Z.B. Maksić, J. Organomet. Chem. 524 (1996) 107.

[8] (a) P. George, M. Trachtmann, C.W. Bock, A.M. Brett, J. Chem. Soc. Perkin Trans. 2 (1976) 1222. (b) P. George, M. Trachtmann, C.W. Bock, A.M. Brett, Tetrahedron 32 (1976) 317.

[9] See for example: J.K. Labanowski, J.W. Andzelm (Eds.), Density Functional Methods in Chemistry, Springer, New York, 1991. J.M. Seminario (Ed.), Recent Developments and Applications of Modern Density Functional Theory, Elsevier, Amsterdam, 1996.
[10] A.D. Becke, J. Chem. Phys. 98 (1993) 1372; 5648.
[11] W.J. Hehre, L. Radom, P.v.R. Schleyer, J.A. Pople, in: Ab initio Molecular Theory, Wiley, New York, 1986 and references cited therein.
[12] Gaussian 94, Revision C.2, M.J. Frisch, G.W. Trucks, H.B. Schlegel, P.M.W. Gill, B.G. Johnson, M.A. Robb, J.R. Cheeseman, T. Keith, G.A. Petersson, J.A. Montgomery, K. Raghavachari, M.A. Al-Laham, V.G. Zakrzewski, J.V. Ortiz, J.B. Foresman, J. Cioslowski, B.B. Stefanov, A. Nanayakkara, M. Challacombe, C.Y. Peng, P.Y. Ayala, W. Chen, M.W. Wong, J.L. Andres, E.S. Replogle, R. Gomperts, R.L. Martin, D.J. Fox, J.S. Binkley, D.J. Defrees, J. Baker, J.P. Stewart, M. Head-Gordon, C. Gonzalez, J.A. Pople, Gaussian, Pittsburgh PA, 1995.
[13] GAMESS, M.W. Schmidt, K.K. Baldridge, J.A. Boatz, S.T. Elbert, M.S. Gordon, J.H. Jensen, S. Koseki, N. Matsunaga, K.A. Nguyen, S.J. Su, T.L. Windus, M. Dupuis, J.A. Montgomery, J. Comput. Chem. 14 (1993) 1347–1363.
[14] W. Koch, M. Eckert-Maksić, Z.B. Maksić, J. Chem. Soc. Perkin 2 (1993) 2195.
[15] O. Mo, M. Yañez, M. Eckert-Maksić, Z.B. Maksić, J. Org. Chem. 60 (1995) 1638.
[16] L. Moore, R. Lubinski, M.C. Baschky, G.D. Dahlke, M. Hare, T. Arrowood, Z. Glasovac, M. Eckert-Maksić, S.R. Kass, J. Org. Chem. 62 (1997) 7390.
[17] J.Y. Lee, O. Hahn, S.J. Lee, H.S. Choi, H. Shim, B.J. Mhin, K.S. Kim, J. Phys. Chem. 99 (1995) 1913.
[18] M. Kotranek, H. Liscka, J. Karpfen, J. Chem. Phys. 96 (1992) 982.
[19] L.S. Bartell, E.A. Roth, C.D. Hollowell, K. Kuchitsu, J.E. Young, J. Chem. Phys. 42 (1965) 2683.
[20] W. Hougen, M. Traetteberg, Acta Chem. Scand. 20 (1966) 1726.
[21] K. Kuchitsu, T. Fukuyama, Y. Mosher, J. Mol. Struct. 1 (1967) 463.
[22] K. Tamagawa, T. Iijima, M. Kimura, J. Mol. Struct. 30 (1976) 243.
[23] W.M. Stigliani, V.W. Laurie, J.C. Li, J. Chem. Phys. 62 (1975) 1890.
[24] (a) W.H. Mills, I.G. Nixon, J. Chem. Soc. (1930) 2150. (b) See also L.E. Sutton, L. Pauling, Trans. Farad. Soc. (1935) 939.
[25] Z.B. Maksić, D. Kovaček, M. Eckert-Maksić, M. Böckman, M. Klessinger, J. Phys. Chem. 99 (1995) 6410.
[26] (a) W. Koch, M. Eckert-Maksić, Z.B. Maksić, Int. J. Quantum Chem. 48 (1993) 319. (b) Z.B. Maksić, M. Eckert-Maksić, M. Hodošček, W. Koch, D. Kovaček, in: Z.B. Maksić, M. Eckert-Maksić (Eds.), Molecules in Natural Science and Medicine, Ellis Horwood, Chichester, 1991, 333.
[27] H. Günther, W. Herrig, The rehybridization effect is rather nicely reflected in the one-bond J(CC) spin–spin coupling constants as shown by NMR measurements, J. Am. Chem. Soc. 97 (1975) 5594.
[28] M. Eckert-Maksić, Z. Glasovac, Z.B. Maksić, I. Zrinski, J. Mol. Struct. (Theochem) 366 (1996) 173.
[29] Z.B. Maksić, M. Eckert-Maksić, K.H. Pfeifer, J. Mol. Struct. 300 (1993) 445.
[30] R.F.W. Bader, Atoms in Molecules: A Quantum Theory, Oxford University Press, New York, 1990.
[31] For a critical analysis and meaning of atomic charges in molecules see: K. Jug, Z.B. Maksić, in: Z.B. Maksić (Ed.), Theoretical Models of Chemical Bonding 3, Springer Verlag, Berlin, 1991, 235.
[32] (a) M. Eckert-Maksić, Z.B. Maksić, M. Klessinger, Int. J. Quantum Chem. 49 (1994) 383. (b) M. Eckert-Maksić, Z.B. Maksić, M. Klessinger, J. Chem. Soc. Perkin Trans. 2 (1994) 285. (c) M. Eckert-Maksić, M. Klessinger, D. Kovaček, Z.B. Maksić, J. Phys. Org. Chem. 9 (1996) 269.
[33] M. Eckert-Maksić, W.M.F. Fabian, R.J. Janoschek, Z.B. Maksić, J. Mol. Struct. (Theochem) 338 (1995) 1.
[34] (a) A.G. Davies, K.M. Ng, J. Chem. Soc. Perkin Trans. 2 (1992) 1875. (b) D.V. Avila, A.G. Davies, E.R. Li, K.M. Ng, J. Chem. Soc. Perkin Trans. 2 (1993) 335.
[35] A.G. Davies, G. Gescheidt, K.M. Ng, M.K. Shepard, J. Chem. Soc. Perkin Trans. 2 (1994) 2423.
[36] A. Martinez, M.L. Jimeno, J. Elguero, A. Fruchier, New J. Chem. 18 (1994) 269.
[37] (a) M. Ramos, I. Alkorta, J. Elguero, Tetrahedron 53 (1997) 1403. (b) I. Alkorta, J. Elguero, Struct. Chem. 8 (1997) 189.
[38] (a) R. Taylor, J. Chem. Soc. Perkin Trans. 2 (1992) 3. (b) P.W. Fowler, D.J. Collins, S.J. Austin, J. Chem. Soc. Perkin Trans. 2 (1992) 275.
[39] W.I.F. David, R.M. Iberson, J.C. Matthewman, K. Prassides, T.J. Dennis, J.P. Hare, H.W. Kroto, R. Taylor, D.R. Walton, Nature 353 (1991) 147.
[40] K. Hedberg, L. Hedberg, D.S. Bethune, C.A. Brown, H.C. Dorn, R.D. Johnson, M. DeVries, Science 254 (1991) 410.
[41] (a) A. Stanger, N. Ashkenazi, R. Boese, P. Stellberg, J. Organomet. Chem. 542 (1997) 19. (b) H. Butenschön, B. Gabor, R. Mynott. H.G. Wey, Z. Naturforsch. 50b (1995) 483.